Emission of Li^8 Fragments from Cu, Ag, and Au Irradiated by High-Energy Protons*

S. KATCOFF AND E. W. BAKER
Chemistry Department, Brookhaven National Laboratory, Upton, New York

AND

N. T. PORILE†
Chemistry Department, Brookhaven National Laboratory, Upton, New York and Chemistry Department, Purdue University, Lafayette, Indiana

(Received 2 August 1965)

Thin targets of Cu, Ag, and Au were irradiated in a scattering chamber with 2-GeV protons and the Li^8 fragments emitted at various angles were collected in nuclear emulsions. Data were also obtained for Li^8 produced in emulsion irradiated directly by 1- to 3-GeV protons. Results are presented on the energy spectra of Li^8, on the angular distributions, and on the emission cross sections. These are compared with the results of a detailed Monte Carlo calculation in which it was assumed that the Li^8 fragments are evaporated from the excited nuclei remaining after the prompt cascade. There is rough agreement between experiment and calculation for the cross sections, for the peak energies in the spectra, and for some of the spectral shapes. However, the experimental angular distributions are more strongly forward-peaked and the experimental energy spectra in the forward direction are considerably broader than the calculated spectra. Either a substantial fraction of the fragments is emitted by a process other than evaporation, or the emission is by a mechanism intermediate between evaporation and fast fragmentation.

INTRODUCTION

NUMEROUS studies have been made of energy spectra and angular distributions of Li^8 fragments produced by high-energy interaction in nuclear emulsions. These fragments (along with B^8) are easily identified by means of the "hammer tracks" (T tracks) they produce in the photographic emulsion.

Baumann, Braun, and Cüer[1,2] studied the hammer tracks produced when 14- and 25-GeV protons interact with the heavy nuclei of photographic emulsion. They attempted to fit their data with calculated evaporation spectra by using a single nuclear temperature in the range 7–8 MeV, a potential barrier 7–9 MeV, and a forward velocity of the evaporating nucleus of $0.01c$. Agreement was obtained only in the energy range 10–40 MeV.

A similar investigation was carried out by Gajewski *et al.*[3] in which they used 9- and 24-GeV protons. Good agreement between the experimental data and an evaporation calculation was obtained over nearly the entire energy range, but it was necessary to use a very high value of the nuclear temperature, $T=12$ MeV, and a very low value of the potential barrier, $V=3$ MeV. Account was taken of the velocity of the emitting nucleus, of fluctuations in this velocity, and of the effect of the recoiling nucleus. These authors concluded that the values of the parameters that were used "are inconsistent with those predicted by the evaporation theory," and that "these results seem to indicate that a new approach to the interpretation of heavy fragment emission is required."

The production of Li^8 fragments by the interaction of 9-GeV protons with lead nuclei was studied recently by Gajewski, Gorichev, and Perfilov.[4] The method involved sandwiching a thin lead foil between layers of nuclear emulsion. From the broad energy spectrum which was observed, a nuclear temperature of 14.9 MeV and a Coulomb barrier of 9.6 MeV was deduced. These results are comparable with those from the AgBr targets: very high temperature and a very low Coulomb barrier.

Skjeggestad and Sørensen,[5] and Breivik, Jacobsen, and Sørenson[6] analyzed Li^8 spectra obtained from emulsions exposed to cosmic rays and to 4.5-GeV negative pions. The data were in good agreement with evaporation calculations when the following parameters were used: nuclear temperature, 11 MeV; Coulomb barrier, 6 MeV; velocity of the emitting system parallel to the beam, $0.017c$. Mainly because such a high nuclear temperature did not seem reasonable to these authors, they concluded that "the majority of the fragments cannot be emitted in nuclear evaporation processes."

In an earlier investigation[7] similar to the present one, Li^8 energy spectra were obtained at several angles from targets of carbon, aluminum, copper, silver, gold, and uranium irradiated with 2.2-GeV protons. The spectra were compared with the results of evaporation calcula-

* Research performed under the auspices of the U. S. Atomic Energy Commission.
† Work supported in part by U. S. Atomic Energy Commission Contract COO-1505-1.

[1] G. Baumann, H. Braun, and P. Cüer, Compt. Rend. **254**, 1966 (1962).
[2] G. Baumann, H. Braun, and P. Cüer, Phys. Letters **8**, 146 (1964).
[3] W. Gajewski, J. Pniewski, J. Siemińska, J. Suchorzewska, and P. Zieliński, Nucl. Phys. **58**, 17 (1964).
[4] W. Gajewski, P. A. Gorichev, and N. A. Perfilov, Zh. Eksperim. i Teor. Fiz. **47**, 1178 (1964) [English transl.: Soviet Physics—JETP **20**, 795 (1965)].
[5] O. Skjeggestad and S. O. Sørensen, Phys. Rev. **113**, 1115 (1959).
[6] F. O. Breivik, T. Jacobsen, and S. O. Sørensen, Phys. Rev. **130**, 1119 (1963).
[7] S. Katcoff, Phys. Rev. **114**, 905 (1959).

tions in which account was taken of the distribution of nuclear temperatures of the parent nuclei emitting the Li^8 fragments, and in which an energy-dependent Coulomb barrier was assumed. The agreement between calculation and experiment was not good; therefore it was concluded that another mechanism in addition to evaporation was needed to completely describe Li^8 emission.

In the previous experiments[7] the Li^8 spectrum from copper seemed to be displaced to higher energies in relation to the spectra from other targets. Since this anomalous result was difficult to understand it was decided to remeasure the spectra and angular distributions from copper, silver, and gold with an improved technique. The results from silver and gold are in excellent agreement with the earlier data,[7] but the Li^8 spectra now observed from copper are at lower energies than previously. The evaporation calculations are also considerably improved in the present work.

EXPERIMENTAL

The experiments reported in this paper have been advanced in several important respects over the previous ones.[7]

1. The target and photographic emulsions were set in an evacuated scattering chamber with 7.6-cm diam, 0.008-cm thick, Mylar windows (Fig. 1). The external beam of the Cosmotron was passed through three quadrupole magnets, a brass collimator, and two more quadrupole magnets before it was focused at the target. Most of the beam was contained in an area of 0.8 cm $\times$2.5 cm, while the target was in the form of a ribbon 0.6 cm$\times$7.6 cm. The nuclear emulsions in the chamber were Ilford K.0, 200 μ thick, and they were arranged at various angles around the target.

2. Three of the four emulsion plates subtended the same solid angle so that angular distributions could be obtained directly without the necessity for normalization.

3. The secondary particles from the target entered three of the emulsions at a dip angle of 15°$\pm$3°. In the fourth plate (see Fig. 1) the dip angle was set at 45°$\pm$5° so that the ends of the shorter tracks would not lie so close to the surface of the emulsion. Track identification is less reliable very near the surface because part of the "hammer head" may leave the emulsion, the sensitivity may be lower there, and the density of background grains may be higher. The significance of these effects may be evaluated by exposing two plates in a single run at both a small and a large dip angle. This study was of special importance as the previous work showed a strong deficiency of low-energy Li^8 particles in the spectra from copper targets.

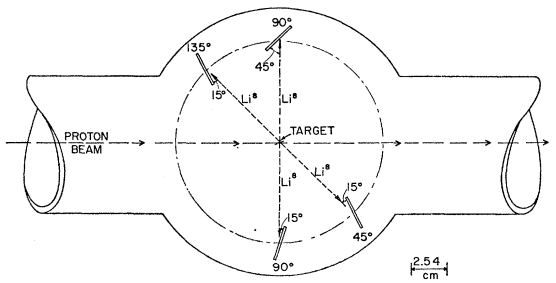

FIG. 1. Scattering chamber showing arrangement of target foil and four nuclear emulsions.

4. The integrated intensity of the beam during each run was determined in order to measure the cross section for production of Li^8. The gross radioactivity induced in each target was measured with a beta proportional counter. This was then compared with the activity of a similar target foil irradiated together with an aluminum monitor foil. Irradiation and counting times, methods of counting, and thickness of targets were matched in the two types of irradiation. The Na^{24} activity produced in the aluminum monitor was determined with a calibrated beta-ray counter. The cross section for this monitor reaction[8] was taken as 9.5 mb at 2.0 GeV.

The duration of each run was 30–60 min and the emulsions were processed soon thereafter in order to minimize fading of the latent image. The method used was the same as that described before.[7] The plates were area scanned and each track selected had the following characteristics: It showed a "hammer head" with two nearly equal and collinear parts, it was at least 5 μ long, it started at the emulsion surface, and it was oriented in such a way that it could have originated in the target. Very few tracks were found which were not so oriented. In one experiment (run as a blank) where the target was omitted, the background of stray tracks was found to be negligible.

Identification as a hammer track was unambiguous in about 90% of the events. Each doubtful case was very carefully examined several times by two or three observers before a decision was made. The recording efficiencies were determined by multiple scanning of the plates. The mean efficiency was 85%. For each hammer track, the coordinates, length, projected angle, and dip angle were recorded.

In addition to the data on Cu, Ag, and Au, results on AgBr, accumulated in the course of other work,[9–11] have also been included. These are from a large number of stars produced in Ilford K.0 emulsion irradiated with 1-, 2-, and 3-GeV protons. The low-energy part of the Li^8 spectra obtained in this way are not subject to any surface effect or self-absorption effect. Li^8 energies can be easily measured down to a fraction of one MeV. Also, data for the angular distribution can be obtained continuously between 0° and 180°. On the other hand, it was necessary to make substantial geometrical corrections for Li^8 tracks leaving the emulsion.

[8] J. B. Cumming, Ann. Rev. Nucl. Sci. **13**, 261 (1963).
[9] E. W. Baker, S. Katcoff, and C. P. Baker, Phys. Rev. **117**, 1352 (1960).
[10] E. W. Baker and S. Katcoff, Phys. Rev. **123**, 641 (1961).
[11] E. W. Baker and S. Katcoff, Phys. Rev. **126**, 729 (1962).

RESULTS

The measured lengths of the tracks were converted to energies by means of the range-energy relations given by Barkas[12] and by Livesey[13] for Li^8 fragments in nuclear emulsion. A correction, 5–7 μ emulsion equivalent, was made for self-absorption in the targets (Table I). No

TABLE I. Summary of data used to obtain the energy spectra at various angles.

Target	Target thickness (mg/cm^2)	Beam energy (GeV)	Lab angle to beam	No. of tracks measured
Cu	3.5	2.2	45°±3°	356
			90°±5°	213
			135°±3°	242
Ag+Br	···	1.0–3.0	0°–180°	431
Ag	3.7	2.0–2.2	45°–55°	468
		2.0	90°±5°	303
		2.0–2.2	125°–135°	360
Au	6.1	2.0–2.2	35°–55°	531
			125°–145°	337

attempt was made to separate tracks due to B^8 from those due to Li^8. This can only affect the results to a very minor degree because the B^8/Li^8 ratios are small[14] and the range distribution of B^8 fragments is expected not to differ much from that of Li^8. Most Li^9 tracks were excluded in the scanning as the alpha tracks of the "hammer head" are, in general, not collinear.

Energy spectra derived from these measurements are shown as histograms in Figs. 2–5. In the interval 5–7.5 MeV, the observed number of tracks was corrected for loss due to self-absorption in the target. Because of the difficulty in identifying short tracks near the surface of the emulsion, the data are less reliable below 10 MeV and no results at all can be given below 5 MeV (for external targets). However, the loss of events from the low-energy portions of these spectra is small as seen by comparison of the Li^8 spectra from external targets of copper and silver with the Li^8 spectra from the Ag and Br in the emulsion (Fig. 5). When the Li^8 energy exceeded 100 MeV some tracks were lost, in the case of 15° dip angle, because they passed through the 200-μ thick emulsion. In the two plates where the dip angle was 45°, tracks were lost when the Li^8 energy exceeded 55 MeV. Account was taken of this fact when combining the data from these plates with those from plates where the dip angle was 15°.

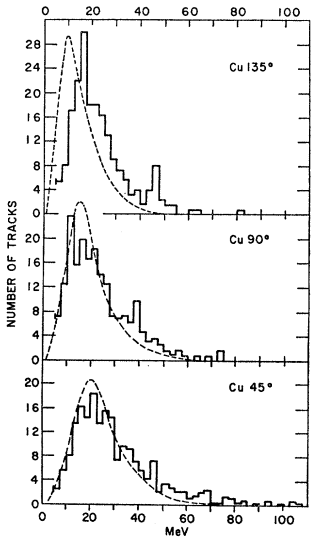

FIG. 2. Energy spectra of Li^8 emitted from copper at 45°, 90°, and 135° to the beam. Histograms–experiment; dashed curves–calculation. All normalized to same area.

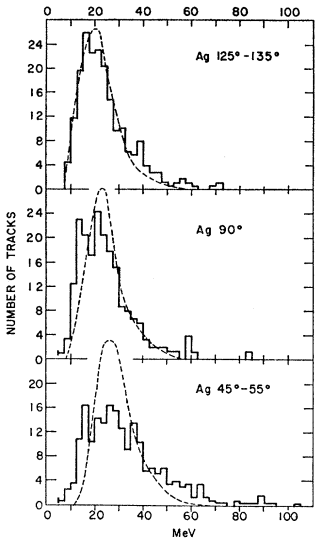

FIG. 3. Energy spectra of Li^8 emitted from silver at forward, sidewise, and backward angles relative to the beam. Histograms–experiment; dashed curves–calculation. All normalized to same area.

The Li^8 energy spectra from silver and gold targets obtained in the present work are in excellent agreement with those reported earlier.[7] Therefore, in order to improve the statistical accuracy, the energy spectra obtained at forward and backward angles in the new experiments were combined with those obtained before. Table I shows the beam energies, angular spread, and the number of tracks measured for each of the spectra. Data at 90° are only from the present work and are taken from plates where the dip angles are 15° and 45°.

The Li^8 energy spectra from copper targets differ considerably from those found in the earlier work.[7] The peaks of the distributions are now at substantially lower energies than previously and they are in reasonable relationship with the results from heavier targets. The precise reason for the discrepancy has not been established, but it seems to be associated with the difficulty of identifying short tracks near the surface of the emulsion. The new data are based on the careful area scanning of seven plates. Nearly all were scanned by each of two scanners. All doubtful tracks were carefully re-examined. The spectrum obtained from the 90° plate, 15° dip, was

[12] W. H. Barkas, Phys. Rev. **89**, 1019 (1953).
[13] D. L. Livesey, Can. J. Phys. **34**, 203 (1956).
[14] See discussion below as well as Refs. 1, 3, 5, and 6.

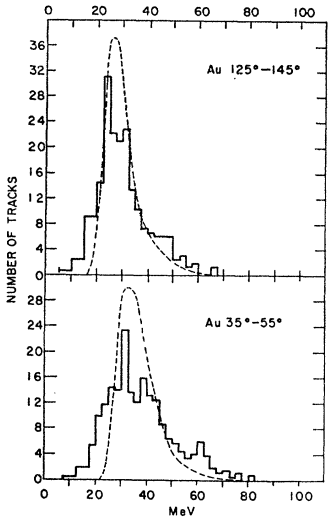

FIG. 4. Energy spectra of Li^8 emitted from gold at forward and backward angles relative to the beam. Histograms–experiment; dashed curves–calculation. All normalized to same area.

identical, within statistics, with the spectrum from the 90° plate, 45° dip. With the greater dip angle short tracks are less likely to be lost, since the hammer heads are not so near the surface of the emulsion.

Angular distributions of the Li^8 fragments from the various targets are shown in Fig. 6. For these results only the data from the present work are included. Only for the case of AgBr are there data at all angles. The forward peaking is greatest for the copper targets and least for gold targets. Observed ratios of Li^8 intensity at 45° to the intensity at 135° are shown in Table II. Comparison with calculation will be discussed below.

The total number of protons passing through the target, in each run, is shown in Table III, column 3. From the known target thicknesses and integration of the hammer-track intensities over 4π solid angle, the production cross sections were estimated. These are listed in column 4, Table III. Because of the uncertainties of the integrations the accuracy is limited to about 35%. Agreement is good with the previous rough estimate.[7] Since the ratio of B^8 to Li^8 production is expected to be small,[14] the cross sections given are essentially those for Li^8.

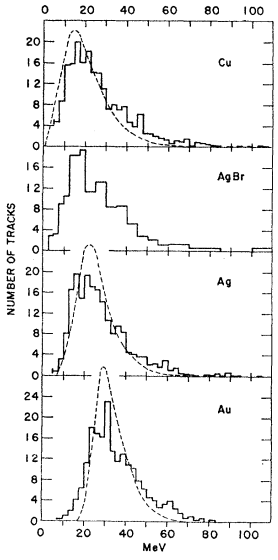

FIG. 5. Energy spectra of Li^8 emitted from copper, silver bromide, silver, and gold. See Table II for details. Histograms–experiment; dashed curves–calculation. All normalized to same area.

TABLE II. Comparison of experimental and calculated forward-to-backward ratios ($N_{45°}/N_{135°}$).[a]

Target	All events		$(E \leq E_{peak})$[b]		$(E > E_{peak})$[c]	
	Experiment	Calc.	Experiment	Calc.	Experiment	Calc.
Cu	2.6	1.9	1.5	0.77	3.6	4.2
Ag	2.4	1.5	1.4	0.86	4.2	3.9
Au	2.0	1.2	0.82	0.59	2.4	2.8

[a] ($N_{45°}/N_{135°}$)—ratio of the number of fragments emitted at 45° to that emitted at 135° to the beam.
[b] Fragments with energy less than the corresponding over-all peak energies (Fig. 5).
[c] Fragments with energy greater than the corresponding over-all peak energies (Fig. 5).

TABLE III. Conditions of irradiation in the new set of experiments and the cross sections for emission of Li^8.

Target	Beam energy (GeV)	Integrated beam intensity	Li^8 cross section (mb) Experiment	Li^8 cross section (mb) Calc.[a]
Cu	2.2	13.5×10^{12}	1.3_3	
Cu	2.2	4.4	1.8_7	
Cu (mean)	2.2		1.6	3
Ag	2.0	6.6	2.8	5
Au	2.0	2.3	6.9	20

[a] Calculated for 1.8-GeV beam energy.

COMPARISON WITH EVAPORATION CALCULATIONS

In this section the experimental results will be compared with theory. We assume that the reactions leading to the emission of Li^8 fragments can be described by the

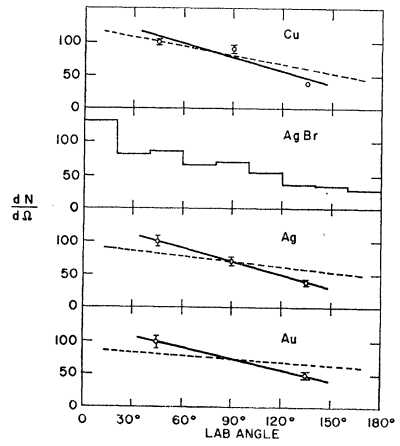

FIG. 6. Angular distributions to the beam of Li^8 emitted from various targets. Points and solid lines–experiment; dashed lines–calculation.

cascade-evaporation formalism. The cascade process involves the prompt emission of nucleons and pions and leads to a spectrum of excited residual nuclei. It is assumed that Li^8 fragments are not emitted during this phase of the reaction. The residual nuclei de-excite by the evaporation of particles. The emission of Li^8 (and B^8) fragments is assumed to occur during this phase of the reaction in competition with that of lighter particles.

The calculation is similar to a previous analysis of α-particle emission and a detailed description is given in that study.[15] The following is an outline of the present treatment.

The distribution of excited nuclei resulting from the cascade process was obtained from the calculation by Metropolis *et al.*[16] The latter gives the values of the atomic number Z, mass number A, and excitation energy E^*, of the residual nuclei. The momentum, p, imparted to these residual nuclei by the cascade process was obtained from Porile's[17] extension of the Metropolis calculation. Cascade results were available for the interaction of 1.8-GeV protons with Cu^{64}, Ru^{100}, and Bi^{209}. The Cu^{64} data were used directly for comparison with the copper results. The distributions of residual nuclei for Ru^{100} and Bi^{209} were appropriately shifted in Z and A to correspond to silver and gold targets, respectively. Small adjustments were also made in the E^* values to account for the calculated dependence of the average excitation energy on target A. The number of available cascade events ranged from approximately 400 for silver to 900 for copper.

The residual nuclei obtained from the cascade calculation were used as the starting nuclei for a Monte Carlo evaporation calculation. The basic formalism was that developed by Dostrovsky *et al.*[18] The high-energy approximation of the level density, $\omega(E)=C\exp[2(aE)^{1/2}]$, was used with a level density parameter $a=A/10$. Two principal modifications were introduced to make this treatment applicable to the present case. As it was desired to obtain energy spectra in the laboratory system, account had to be taken of the motion of the emitting nuclides. A previously developed procedure[15,19] was used for this purpose. It has been shown that the velocity V_{L_n} in the laboratory system of the nth particle emitted in a particular evaporation chain is given by

$$\mathbf{V}_{L_n}=[2M_{R_n}E_n/M_{P_n}(M_{R_n}+M_{P_n})]^{1/2}\mathbf{u}+\sum_{i=1}^{n-1}\mathbf{v}_i+\mathbf{v}_c, \quad (1)$$

where M_{R_n} is the mass of the residual nucleus resulting from the evaporation of n particles, M_{P_n} is the mass of the nth evaporated particle, E_n is the channel energy for the nth evaporation step, $\mathbf{v}_i$ is the recoil velocity due to the evaporation of the ith particle, $\mathbf{v}_c$ is the velocity acquired by the residual nucleus in the cascade process, and $\mathbf{u}$ is a unit vector. The direction of motion of the evaporated particle is obtained by the choice of two random numbers on the assumption of isotropic emission in the system of the emitting nucleus. This condition determines the direction of $\mathbf{u}$ and $\mathbf{v}_i$, and thereby permits the evaluation of Eq. (1). The differential energy spectrum for a given particle follows immediately.

The second modification introduced in the present calculation relates to the fact that the probability of Li^8 emission is very low. The usual Monte Carlo method is therefore not practical as the calculation of Li^8 energy spectra would require an inordinately large amount of computer time. A modification similar to that used by Dostrovsky *et al.*[20] in the calculation of cross sections for light-fragment production was introduced to overcome this difficulty. The usual Monte Carlo treatment in which any one of the six lightest particles (n, p, d, t, He^3, or He^4) can be emitted was retained. In addition, at each step of the de-excitation process the emission probability, energy in the laboratory system, and direction of motion of Li^8 (and B^8) were computed in the customary way. The energy spectrum of Li^8 fragments[21] was then obtained from the laboratory energies weighted by the corresponding emission probabilities, i.e.,

$$N(\Delta E_j)=\sum_n\sum_i P_{ni}(\Delta E_j), \quad (2)$$

where P_{ni} is the total probability for the emission of Li^8 in the ith evaporation step for the nth starting nucleus and ΔE_j is a particular 2.5-MeV-wide energy bin. Since the emission angle relative to the direction of the incident proton was recorded, differential energy spectra could be obtained for comparison with the experimental results obtained at specific angles.

The evaporated Li^8 and B^8 fragments can be formed either in their ground or in bound excited states. For instance, Li^8 has states at 0.98 and 2.26 MeV that are known to decay to the ground state.[22] As far as the evaporation calculation is concerned, these states must be considered as separate entities having their own emission probabilities. Although the inclusion of bound excited states has a substantial effect on the calculated cross sections, the effect on the energy spectra is completely negligible. Therefore, in order to conserve computer time, only ground-state emission of Li^8 and B^8 was considered in detail. The effect of excited-state

[15] N. T. Porile, Phys. Rev. **135**, B371 (1964).
[16] N. Metropolis, R. Bivins, M. Storm, J. M. Miller, G. Friedlander, and A. Turkevich, Phys. Rev. **110**, 204 (1958).
[17] N. T. Porile, Phys. Rev. **120**, 572 (1960).
[18] I. Dostrovsky, Z. Fraenkel, and G. Friedlander, Phys. Rev. **116**, 683 (1959).
[19] N. T. Porile and S. Tanaka, Phys. Rev. **135**, B122 (1964).
[20] I. Dostrovsky, Z. Fraenkel, and J. Hudis, Phys. Rev. **123**, 1452 (1961).
[21] B^8 fragments were excluded from the calculated energy spectra because the experimental spectra as determined here are hardly affected by the presence of a small B^8 component. However, B^8 emission was included in the cross-section and angular-distribution calculations.
[22] T. Lauritsen and F. Ajzenberg-Selove, in *Nuclear Data Sheets*, compiled by K. Way *et al.* (Printing & Publishing Office, National Academy of Sciences–National Research Council, Washington 25, D. C.) NRC [61-5,6-49].

emission was, however, treated in an approximate way in order to retain the correct relative evaporation probabilities of Li^8 and B^8 as well as to permit an approximate estimation of cross sections. The procedure used was simply to increase the statistical weights of Li^8 and B^8 by factors of 2 and 1.2, respectively. These values are based on a few computations in which the emission probabilities of the excited nuclei were compared with those of the corresponding ground-state nuclei.

The present treatment neglects the emission of excited progenitors of Li^8, such as Li^9 and Be^9, which decay to the former by nucleon evaporation. Although this secondary evaporation process appears to make a significant contribution to the production cross sections of light fragments,[23] its effect on their energy spectra is expected to be much smaller. This has been demonstrated in the case of Na^{24} emission.[24] An approximate calculation of the spectrum of Li^8 fragments resulting from the decay of excited Li^9 was performed to check this point. This spectrum was obtained on the basis of a single starting nucleus Ru^{100} with 300-MeV excitation energy. It was found that this spectrum was slightly broader than that for directly produced Li^8 fragments. In view of the small magnitude of this difference no consideration was given to this effect in the detailed calculations presented here.

The calculated energy spectra of evaporated charged particles are rather sensitive to the form of the expression for the inverse reaction cross section. The evaporation formalism of Dostrovsky *et al.*[18] uses the sharp cutoff approximation

$$\sigma_r=\pi R^2(1+c)(1-kV/E), \tag{3}$$

where c and k are constants that depend on the identity of the emitted particle and on target A, and V is the classical Coulomb barrier. The previous calculation of α-particle spectra[15] has shown that satisfactory agreement with experiment can be obtained by use of Eq. (3) provided that the constants are adjusted to give a fit to spectra from compound nuclear reactions. Since no adequate data on the emission of Li^8 fragments in low-energy reactions are available, this fitting procedure could not be used. Instead, the constants were chosen by interpolation between the α-particle values and those for C^{12} and heavier fragments. The calculation of Thomas[25] indicates that in the case of the latter the probability of barrier penetration is negligibly small. The values of k chosen for Li^8 and B^8 were 0.90 and 0.95, respectively, for all A values. The constant c was set equal to zero. The Coulomb barrier was taken as

$$V=Z_1Z_2e^2/r_0(A_1^{1/3}+A_2^{1/3}), \tag{4}$$

with $r_0=1.5$ F.

Two evaporation calculations were performed for each starting cascade product nucleus in order to sample various possible de-excitation paths. The results of the calculation were obtained in the form of differential energy spectra over angular intervals appropriate for comparison with experiment.

The calculated and experimental differential energy spectra are compared in Figs. 2–5. The calculated curves include all fragments emitted at angles of 40°–50°, 85°–95°, and 130°–140° to the beam. The two sets of spectra have been normalized to each other. We shall first discuss the spectra integrated over all of the above angles (Fig. 5).

The comparison reveals both areas of agreement and of disagreement. The calculated peak energies are seen to agree closely with the corresponding experimental values for all three targets. In all cases the peaks occur a few MeV above the classical Coulomb barrier for Li^8 emission from the target nucleus.

The calculated spectra differ in shape from the experimental ones. The statistical significance of these discrepancies was checked with a χ^2 test, and it was found that the differences are real at a confidence level in excess of 99%. It can be seen that the shapes differ at both the high- and low-energy ends of the spectra. The calculation thus underestimates the emission probability of high-energy fragments. The ratio of the observed to the calculated number of fragments with energies exceeding the most probable calculated energy by more than a factor of 2, ranges from 2.0 ± 0.4 for copper to 4.7 ± 1.8 for gold.

A systematic trend with target A may be noted in the comparison of the low-energy ends of the spectra. In the case of copper the calculated number of low-energy fragments is larger than the experimental value. The low-energy portions of the spectra are in good agreement for silver. The situation is reversed in the case of gold and now the calculation significantly underestimates the emission of low-energy fragments. It is important to note that this trend cannot be due to the sharp cutoff approximation to the inverse reaction cross section. In order to bring experiment and calculation into agreement, k would thus have to decrease with increasing A. This would be contrary to the known A dependence of the probability for barrier penetration. While better agreement for gold could of course be obtained by reducing k, this would be at the expense of the fit obtained for the other targets. The present choice of k gives as good an over-all agreement with experiment as any other value and, in addition, is consistent with the systematic trend of barrier penetrabilities noted for other particles.

It is worth noting at this point that the above discrepancies would be considerably more severe if proper account had not been taken of the motion of the emitting nuclei. This is indicated in Fig. 7 where the laboratory-system spectrum calculated for silver is compared with that obtained for the system of the moving

[23] I. Dostrovsky, R. Davis, Jr., A. M. Poskanzer, and P. L. Reeder, Phys. Rev. **139**, B1513 (1965).
[24] N. T. Porile (to be published).
[25] T. D. Thomas, Phys. Rev. **116**, 703 (1959).

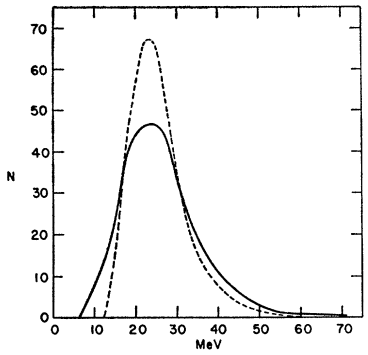

FIG. 7. Effect of the motion of the emitting nuclei on the calculated energy spectrum of Li^8 from silver. Solid curve–laboratory system; dashed curve–system of the moving emitting nuclei.

nuclei. This calculation was performed by setting $\mathbf{v}_c$ and $\sum \mathbf{v}_i$ in Eq. (1) equal to zero. It is seen that the inclusion of center-of-mass motion considerably broadens the calculated spectrum. This is particularly noticeable for the low-energy fragments. The latter arise from the partial cancellation of the generally forward-directed cascade momentum and that of moderately low-energy fragments that happen to be emitted in the backward direction. On the other hand, the highest energy fragments arise from the addition of the cascade momentum to that of already energetic Li^8 fragments emitted in the forward direction.

In order to examine the above-mentioned discrepancies in more detail, it is worth looking at some additional features of the results. The differential energy spectra at 45°, 90°, and 135° are compared with calculation in Figs. 2–4. The experimental spectra are broader than the corresponding calculated ones, especially in the forward direction. The experimental angular distributions are compared with calculation in Table II and in Fig. 6. For all targets the distribution is more forward-peaked than predicted by the calculation.

A possible explanation for these discrepancies is the assumption that the high-energy Li^8 are emitted in the course of the knock-on cascade as a result of fragmentation. It is then reasonable to expect these fragments to partake of the directional characteristics and energy of the incident proton. Table II indicates that the high-energy Li^8 are indeed predominantly emitted in the forward direction. It is of interest to note that the calculation predicts equally large values of $N_{45°}/N_{135°}$. The latter are due, of course, to the forward motion of the residual nuclei resulting from the knock-on cascade. It is thus apparent that the forward-to-backward ratio of energetic fragments is not very sensitive to the mechanism of their production. A similar conclusion was previously drawn in the analysis of α-particle spectra.[15]

The calculated values of $N_{45°}/N_{135°}$ for low-energy fragments are seen to be significantly less than unity. The predominantly backward emission of these fragments in the laboratory system lends corroboration to the previous statement that they arise from the partial cancellation of cascade and evaporation momenta. The experimental values of $N_{45°}/N_{135°}$, while much lower than the corresponding values for high-energy fragments, are nearly a factor of 2 larger than calculation. This difference suggests that directional effects may be connected with the discrepancy in the low-energy portions of the spectra. This is also apparent in Figs. 2–4, which show that the peak positions in the backward spectra differ considerably more from the experimental values than those in the forward spectra. The calculated peak energy at 135° for copper thus is some 6 MeV less than the experimental value while that for gold is about 4 MeV larger than the latter. We recall that the comparison of the low-energy portions of the over-all spectra (Fig. 5) revealed precisely the same trend. By contrast, the calculated and experimental peak energies of the forward spectra are in better agreement.

A possible explanation for the abundant emission of low-energy fragments is the reduction of the Coulomb barrier at high excitation energies. Several authors[26–30] have postulated that the Coulomb barrier may vary with excitation energy because of the thermal expansion or surface oscillation effects. Although no evidence for this effect was found in the previous study of α-particle emission from AgBr, it is quite possible that barrier reduction may be of importance for Li^8 fragments emitted from heavier targets. The following reasons may be cited: (1) Barrier reduction may be more important in the case of Li^8 emission because the average excitation energy at which this fragment is emitted is larger than that for α-particle evaporation. (2) This effect may be more important in the heavy-element region because of the substantial increase with target A of the average excitation energy. (3) The Coulomb barrier may also be reduced because of distortion effects.[31] The emission of a fragment as massive as Li^8 may require a distortion of the emitting nucleus at the scission point analogous to that encountered in fission. The barrier would thus be lower than that for spheres in contact as given by Eq. (4). To a first approximation, this effect is equivalent to a further reduction of the constant k in Eq. (3). In light of the previous discussion, it is apparent that this effect would have to become more important with increasing target A.

In order to gain further insight into the process of Li^8 emission during high-energy nuclear reactions, the data were transformed to give velocity spectra (Fig. 8). The experimental results are shown as histograms while the results of calculation are given by the dashed curves. It is seen that the calculated velocity spectra, for each target element, have very nearly the same shape and width at each angle; the curves are merely displaced

[26] E. Bagge, Ann. Physik **33**, 389 (1938); Phys. Z. Sowjetunion **44**, 461 (1942).
[27] K. J. Le Couteur, Proc. Phys. Soc. (London) **A63**, 259 (1950).
[28] Y. Fujimoto and Y. Yamaguchi, Progr. Theoret. Phys. (Kyoto) **5**, 76 (1950).
[29] Y. Yamaguchi, Progr. Theoret. Phys. (Kyoto) **5**, 501 (1950).
[30] A. M. Lane and K. Parker, Nucl. Phys. **16**, 690 (1960).
[31] R. Da Silveira, Phys. Letters **9**, 252 (1964).

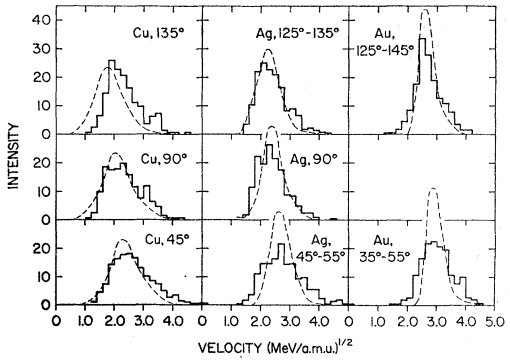

FIG. 8. Velocity spectra of Li^8 emitted from copper, silver, and gold at various angles to the beam. Histograms–experiment; dashed curves–calculation. All normalized to same area.

along the velocity axis. This behavior is consistent with the model that formed the basis of the calculation: a fast nucleon cascade followed by evaporation on a relatively slow time scale. Furthermore, the mean forward velocity imparted to the nucleus during the fast cascade is given by $1/\sqrt{2}$ times the shift of the calculated velocity spectrum between 135° and 45°. In units of $(\text{MeV/amu})^{1/2}$ these velocities are 0.37, 0.30, and 0.19 for copper, silver, and gold, respectively (0.012, 0.010, and 0.006 in units of c). The observed velocity distributions show a forward-backward shift of comparable magnitude. However, the distributions are all broader at the forward angles than at the backward angles suggesting a contribution from another mechanism.

As a final comparison between experiment and calculation we list the cross sections for Li^8 emission in Table III. The calculated values include contributions from B^8 fragments of 14, 7, and 1% for Cu, Ag, and Au, respectively. These values are only approximate because the emission of excited Li^8 and B^8 fragments was not properly treated and the emission of particle unstable progenitors was neglected. The data in Table III indicate that the calculation matches the trend with target A shown by the experimental values, although it does overestimate the latter by about a factor of 2. In view of the above uncertainties this discrepancy should not be taken very seriously.

We conclude from this analysis that conventional evaporation theory can account for some of the features of Li^8 emission in high-energy interactions. These include the trend with target A of the integrated cross sections, the approximate peak positions in the energy spectra, and in some cases, the over-all shapes of the energy spectra. The main shortcomings of the calculation lie in its failure to match the strong forward peaking of the angular distribution and in its inability to account for the emission of the highest energy fragments. These are just the characteristics that lithiums formed as a result of a fast fragmentation process might be expected to have. These fragments, emitted in the course of the knock-on cascade, might be expected to partake of the energy and direction of motion of the incident proton. The present comparison thus suggests that a significant fraction of the Li^8 fragments is emitted as a result of a fast fragmentation rather than a slower evaporation process. Alternatively, the emission of light fragments may take place by a mechanism intermediate between these two extremes.

In a recent paper by Dostrovsky *et al.*,[23] evaporation calculations were performed to compare with measured relative cross sections for production of various light fragments in high-energy reactions. The calculations, with parameters very similar to those used here, reproduced well the observed dependence on mass number and neutron-to-proton ratio of the target. On the other hand, we have shown here that the calculations are not as successful for prediction of energy spectra and angular distribution of the fragments.[32]

ACKNOWLEDGMENTS

We are very grateful to Mrs. Dorothea Hodgdon and Mrs. Doris Franck for their very patient and careful scanning of the emulsions.

[32] In a study of the energy spectrum and angular distributions of Na^{24} fragments emitted from Bi irradiated by 2.9-GeV protons it was shown that the emission is by a rapid process. J. B. Cumming, R. J. Cross, Jr., J. Hudis, and A. M. Poskanzer, Phys. Rev. **134**, B167 (1964).